

## Anisotropic microwave resistance of $\text{YBa}_2\text{Cu}_3\text{O}_{6.95}$ and the modified two-fluid model

Herman J. Fink

*Department of Electrical and Computer Engineering, University of California, Davis, California 95616*

M. R. Trunin

*Institute of Solid State Physics, Russian Academy of Sciences, 142432 Chernogolovka, Moscow District, Russia*

(Received 1 March 2000)

Experiments of the anisotropic microwave surface resistance of  $\text{YBa}_2\text{Cu}_3\text{O}_{6.95}$  crystals by Hosseini *et al.* [Phys. Rev. Lett. **81**, 1298 (1998)] are well described by a modified two-fluid model proposed by the authors. For currents perpendicular to the  $ab$  plane at 22 GHz, the electron-scattering rate  $\tau(T)^{-1}$  is nearly temperature ( $T$ ) independent below the transition temperature  $T_c$ , while for currents in the  $ab$  plane,  $\tau(0)^{-1}$  is approximately two orders of magnitude smaller and constant below  $\sim T_c/4$ , increasing rapidly by two orders of magnitude between  $T_c/4$  and  $T_c$ . The real part of the conductivity  $\sigma'$  has a prominent maximum near 35 K for in-plane currents, while for  $c$ -axis currents  $\sigma'(T)$  decreases rapidly below  $T_c$ .

The modified two-fluid model of the microwave surface impedance  $Z_s = R_s + iX_s$  of cuprates is discussed in Refs. 1–6 with regard to the temperature dependence of  $Z_s(T)$  in the  $ab$  plane for different optimally doped high- $T_c$  single crystals. Here, we apply our model to the anisotropic microwave properties of high-quality single crystals of  $\text{YBa}_2\text{Cu}_3\text{O}_{6.95}$  (YBCO).

The real part of the surface impedance  $\text{Re}[Z_s] = R_s$  is a measure of the microwave power absorbed. With the definition  $s = (\sigma'/\sigma'')^2$ , where  $\sigma'$  and  $\sigma''$  are the real and imaginary parts of the conductivity, the real part of  $Z_s$  is

$$R_s = \sqrt{\frac{\omega\mu_0}{2\sigma''}} \sqrt{\frac{\sqrt{1+s}-1}{1+s}}. \quad (1)$$

The relevant equations describing the microwave impedance of cuprates by the modified two-fluid model, in the notation of Ref. 3, are the following ( $t = T/T_c$ ):

We write for the resistivity

$$\rho_{dc}(t) = \rho_r + \rho_i(1)t^5g(t), \quad (2)$$

where  $\rho_r$  is the inherent residual and  $\rho_i(1)$  the intrinsic resistivity, the latter at  $T_c$ .  $\rho_r$  is temperature independent in the modified two-fluid model,

$$g(t) = f\left(\frac{\Theta_D}{T_c} \frac{1}{t}\right) / f\left(\frac{\Theta_D}{T_c}\right), \quad (3)$$

with  $\Theta_D$  the Debye temperature and

$$f(\Theta_D/T) = \int_0^{\Theta_D/T} \frac{x^5 dx}{(e^x - 1)(1 - e^{-x})}. \quad (4)$$

We define a resistivity ratio  $r = \rho_r/\rho_i(1)$  with  $1/\rho_i(1) = \sigma_i(1) = \sigma_{dc}(T_c)(r+1)$ . The electron scattering time is

$$\tau(t) = \frac{\mu_0\lambda^2(0)\sigma_{dc}(T_c)(r+1)}{r+t^5g(t)}, \quad (5)$$

and the conductivity components ( $\sigma = \sigma' - i\sigma''$ ) are

$$\sigma'(t) = \sigma_{dc}(T_c) \left( \frac{n_n(t)/n}{r+t^5g(t)} \right) \frac{r+1}{1+[\omega\tau(t)]^2}, \quad (6)$$

$$\sigma''(t) = [\omega\mu_0\lambda^2(t)]^{-1} + \omega\tau(t)\sigma'(t). \quad (7)$$

$n_n(t)/n = 1 - [\lambda(0)/\lambda(t)]^2$  is the quasiparticle fraction. The term  $[\omega\mu_0\lambda^2(t)]^{-1} = n_s(t)e^2/m\omega$  arises from the superelectrons and is the dominant term in Eq. (7) at low temperatures.

Experiments that deal with the anisotropy of the microwave surface impedance and complex conductivity of optimally doped YBCO single crystals are listed in Refs. 7–15. Here, we investigate in detail experiments of Hosseini *et al.*<sup>13</sup> at 22 GHz that deal with measurements of the  $T$  dependence of the surface impedance for currents along the  $a$  axis,  $b$  axis, and  $c$  axis of an untwinned single crystal of YBCO. We believe that the data of Ref. 13 are representative of YBCO.

Figure 1 shows the experimental points of  $[\lambda(0)/\lambda(t)]^2$ , taken from Ref. 13, for microwave currents flowing along the  $a$  axis,  $b$  axis, and  $c$  axis of the YBCO crystal. The experimental data fit the following equations. For the  $a$  axis and  $b$  axis,

$$[\lambda(0)/\lambda(t)]^2 \approx 1 - at - (1-a)t^6, \quad (8)$$

and for the  $c$  axis,

$$[\lambda(0)/\lambda(t)]^2 \approx 1 - at^2 - (1-a)t^8. \quad (9)$$

The main difference between Eq. (8) and Eq. (9) is that at low temperatures ( $T \ll T_c$ ), in agreement with experiments<sup>13</sup>, Eq. (8) provides for a linear  $T$  dependence of the  $ab$  plane penetration depth  $[\Delta\lambda_{ab}(T) \propto T]$ , while for currents along the  $c$  axis, Eq. (9) leads to  $\Delta\lambda_c(T) \propto T^2$ . We note that the linear temperature dependence of  $\Delta\lambda_{ab}$  in high-quality YBCO single crystals is generally accepted, contrary to the  $T^2$  dependence of  $\Delta\lambda_c$ . In particular, in the experiments of

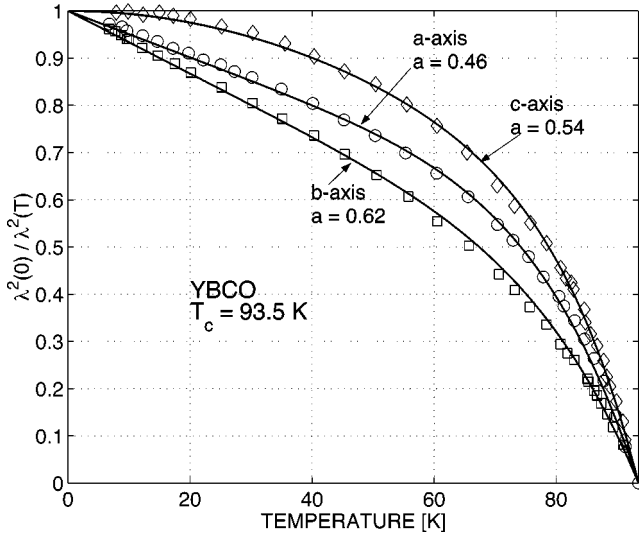


FIG. 1. Equations (8) and (9) showing the fit to the empirical  $[\lambda(0)/\lambda(T)]^2$  as a function of temperature. The experimental points are from Ref. 13, Fig. 2.

Refs. 9 and 11, the low-temperature  $\lambda_c(T)$  exhibits a linear variation contrary to what is observed in Ref. 13.

Figure 2 is a linear plot of the surface resistance  $R_s(T)$ , calculated from Eq. (1), with Eqs. (5)–(7) for the  $a$  axis,  $b$  axis, and  $c$  axis. The parameters used in the calculations are stated in the figure. The  $\lambda(0)$  values of the  $a$  axis and  $b$  axis are compatible with those of Refs. 14 and 15. The  $\lambda(0)$  value for the  $c$  axis was chosen to fit the experimental data of Ref. 13. The experimental points in Fig. 2 are from Fig. 4 of Ref. 13. The overall fit is good, in particular for the  $b$  axis. The experimental data, extrapolated to  $T=0$ , show a small but finite resistance denoted by  $R_0=40 \mu\Omega$ , which was added to the calculated  $R_s(T)$  values obtained from Eq. (1). This resistance is different in nature from the residual resistivity denoted here by  $\rho_r$ . It is not clear what the origin of  $R_0$  is except that its imprint on the measurements is different

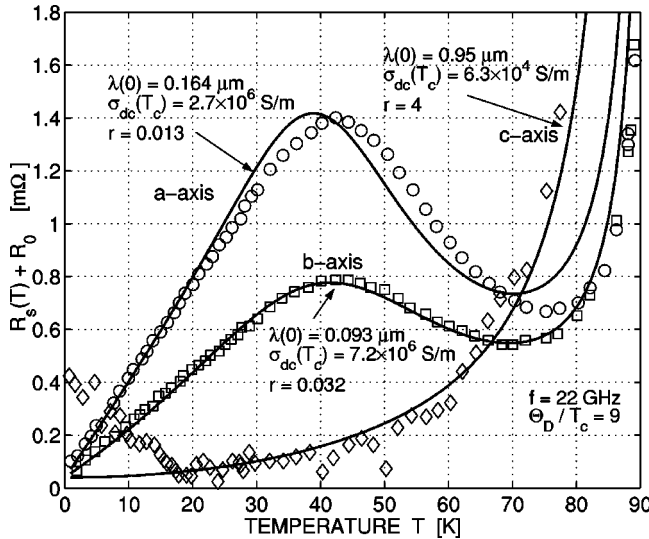


FIG. 2. Linear plot of resistance  $R_s(T)+R_0$  as a function of temperature for the  $a$ ,  $b$ , and  $c$  axes calculated from Eq. (1), all at 22 GHz. The experimental points are from Ref. 13, Fig. 4. We put  $R_0=40 \mu\Omega$  for all three axes.

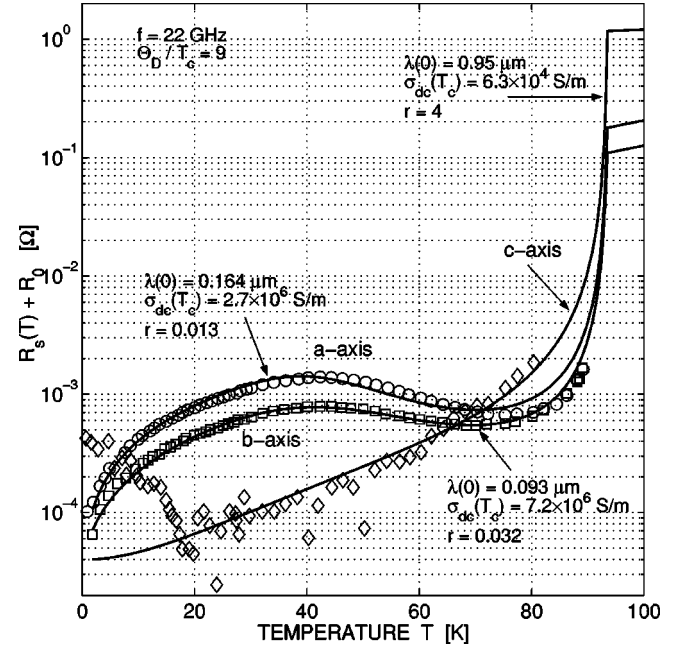


FIG. 3. Semilogarithmic plot of resistance  $R_s(T)+R_0$  as a function of temperature for the  $a$ ,  $b$ , and  $c$  axes, all at 22 GHz with  $R_0=40 \mu\Omega$ .  $R_s(T)$  is calculated from Eq. (1). The experimental points are from Ref. 13.

from that of the residual resistivity  $\rho_r$ . The experimental data of the  $c$  axis stray considerably, and it is unclear if the peak below 20 K is outside the experimental accuracy or if  $R_s(T)$  actually increases with decreasing temperature below 20 K. We shall remark on this peak later.

Figure 3 is the same as Fig. 2 except that  $R_s(T)+R_0$  is plotted on a semilogarithmic scale with the experimental points extracted from Ref. 13. Near  $T_c$ , the surface resistance changes by orders of magnitude and has a discontinuous slope at  $T_c$ , neglecting broadening of the transition due to sample inhomogeneities and/or fluctuations. The plotted curves above  $T_c$  for the  $a$  axis and  $b$  axis are compatible with the experimental data of Ref. 12 but are distinct from the experiments of Ref. 13 and, therefore, are not shown in Fig. 3. For the  $c$  axis, only one value of the resistivity above  $T_c$  is given,<sup>13</sup> which was used to plot the curve above  $T_c$ .

It is possible to calculate  $\sigma'(T)$  from the experimental surface resistance data, using Eq. (1) and Eq. (7) instead of Eq. (6). This procedure is exact not only at low temperatures but also near and above  $T_c$ , provided the superelectron density  $n_s(T)$  is put equal to 0 at and above  $T_c$ . Substituting Eq. (7) into Eq. (1), one obtains a fourth-order polynomial in  $\sigma'(T)$ ,

$$c_4\sigma'^4 + c_3\sigma'^3 + c_2\sigma'^2 + c_1\sigma' + c_0 = 0, \quad (10)$$

with

$$c_5 = (\omega\mu_0)/(2R_{\text{expt}}^2),$$

$$c_0 = [\omega\mu_0\lambda^2(T)]^{-1} \propto n_s(T),$$

$$\nu = \omega\tau(T),$$

$$c_4 = (1 + \nu^2)^2,$$

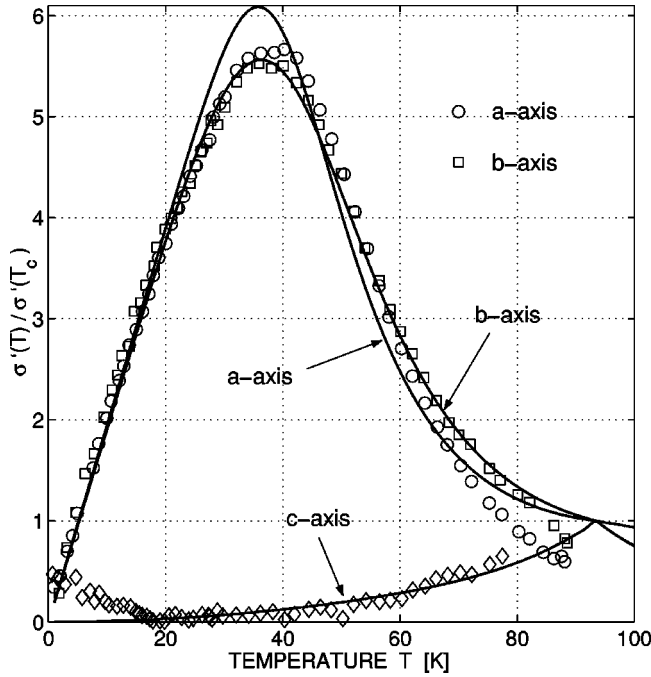


FIG. 4. Linear plot of the real part of the conductivity  $\sigma'(T)$ , normalized by  $\sigma'(T_c)$  for currents flowing along the  $a$  axis,  $b$  axis, and  $c$  axis at 22 GHz. Solid curve obtained from Eq. (6),  $\circ$ ,  $\square$ , and  $\diamond$  from Eq. (10) with  $R_0 = 40 \mu\Omega$  subtracted from  $R_{expt}$  for  $\circ$ ,  $\square$ , and  $\diamond$  data.

$$c_3 = 2\nu(1 + \nu^2)(2\sigma_0 + \sigma_s),$$

$$c_2 = 2(1 + 3\nu^2)\sigma_0(\sigma_0 + \sigma_s) - \sigma_s^2,$$

$$c_1 = 2\nu\sigma_0^2(2\sigma_0 + 3\sigma_s),$$

$$c_0 = \sigma_0^3(\sigma_0 + 2\sigma_s).$$

Equation (10) has two positive roots, one of which is orders of magnitude larger than the physically expected solution. Above  $T_c$ , the value of  $\sigma_0 = 0$  since  $n_s(T) = 0$  for  $T \geq T_c$ .

Figure 4 shows  $\sigma'(T)$ , which was obtained the following way. Measured values of  $T$  and  $R_{expt}$  were taken from Ref. 13. This determines the value of  $\sigma_s$ . One has the choice here to use the actually measured value  $R_{expt}$ , or to subtract from it  $R_0$  if one wants to make a comparison with the value calculated from Eq. (1). Since  $R_0$  is quite small for the experiments under consideration, it makes only a very small difference in the final results if we incorporate  $R_0$  in the present analysis. However, it should be noted that this resistance is different in nature from the residual resistivity denoted here by  $\rho_r$ . It is not clear what the origin of  $R_0$  is except that its imprint on the measurements is different from that of the residual resistivity  $\rho_r$ . Perhaps a universal conductivity limit is reached as  $T \rightarrow 0$  K,<sup>16</sup> or a small number of extraneous impurity carriers remained near  $T = 0$  K. These carriers do not necessarily affect  $\tau(T)$  in our model.

With the measured value of  $T$ , the value of  $\lambda$  is calculated from Eq. (8) or Eq. (9), which specifies  $\sigma_0$  and  $\nu$  [with the help of Eq. (5)]. It is then straightforward to obtain the physical root of  $\sigma'$  from Eq. (10), shown in Fig. 4 for the experimental data points extracted from Ref. 13. The stray of the data points in Fig. 4 is larger for the  $c$  axis than the  $a$  axis or

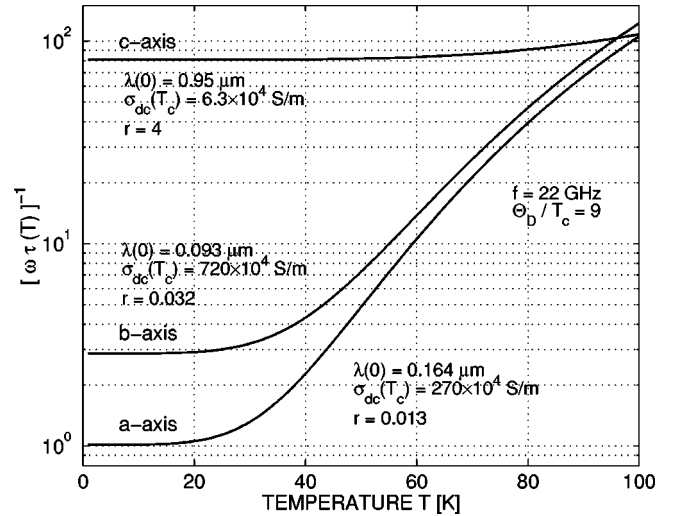


FIG. 5. Semilogarithmic plot of normalized electron-scattering rate  $[\omega\tau(T)]^{-1}$  as a function of temperature for the  $a$ ,  $b$ , and  $c$  axes, calculated from Eq. (5).

$b$  axis. The curves calculated from Eqs. (6) are a good fit to the  $a$  axis,  $b$  axis, and  $c$  axis data, neglecting the low-temperature peak of the  $c$  axis data.

We find the following: Our modified two-fluid model, which is employed here, describes and fits well the experimental data of Ref. 13, although the  $c$  axis data of the surface resistance  $R_s$  and the conductivity  $\sigma'$  look quite different from the  $a$  axis and  $b$  axis data. As can be seen from Fig. 3,  $R_s$  is one order of magnitude larger for the  $c$  axis above  $T_c$  than for the  $a$  axis or  $b$  axis, while below  $T_c/2$  the reverse is true, at least down to approximately 20 K. Whether the  $c$  axis peak of  $R_s$  below 20 K is real or an artifact due to an inaccuracy in the small difference, obtained from subtracting two large numbers, remains an open question. Ignoring this peak, the overall agreement between the experimental data and the proposed two-fluid model is very respectable.

The normalized scattering rate  $[\omega\tau(T)]^{-1}$  as a function of temperature is shown for the three axes in Fig. 5. The experimental parameters that are the key to this model are  $\lambda(T)$ ,  $\sigma_{dc}(T_c)$ , and the resistivity ratio  $r$  relative to the term  $t^5g(t)$  in the electron-scattering time  $\tau$ , Eq. (5). At low temperatures, over the temperature interval where  $r \geq t^5g(t)$ , the slopes of  $R_s$  and  $\sigma'$  are mainly controlled by the temperature dependence of  $\lambda(T)$ , because  $\tau(T) \approx \text{const}$  over this temperature interval. This implies a linear temperature increase of  $R_s(T)$  and  $\sigma'(T)$  for the  $a$  axis and  $b$  axis, while for the  $c$  axis the slopes of  $R_s(T)$  and  $\sigma'(T)$  are zero at low temperatures and, therefore,  $R_s(T)$  and  $\sigma'(T)$  increase considerably less rapidly.

Since two-dimensional conduction in the  $ab$  plane is favored in cuprates, the resistance perpendicular to the  $ab$  plane above  $T_c$  is much larger than the in-plane resistance (see Fig. 3) and gives rise to much larger  $r$  values for the  $c$  axis. Therefore, a constant  $c$  axis electron-scattering rate is predominant because  $r \geq t^5g(t)$  for most temperatures below  $T_c$ , as is seen in Fig. 5 for the  $c$  axis. From this we infer that  $R_s(T)$  and  $\sigma'(T)$  for the  $c$  axis are mainly controlled by the  $c$ -axis  $\lambda$ , except close to  $T_c$ .

For smaller electron-scattering rates by impurities, such as for the  $a$  axis and  $b$  axis, that is, for smaller values of the

resistivity ratio  $r$ , the value of  $r+t^5g(t)$  increases rapidly as the temperature is increased above 30 K. As a consequence,  $R_s(T)$  and  $\sigma'(T)$  decrease above 35 to 40 K.  $R_s(T)$  tends toward a minimum near 65 to 75 K before reaching its much larger normal state value (due to a very rapid decrease of  $\sigma''$  very close to  $T_c$ ), while  $\sigma'(T)$  tends toward  $\sigma_{dc}(T_c)$ .

It is surprising to obtain smaller  $R_s(T)$  values (smaller microwave losses) for currents flowing perpendicular to the  $ab$  plane than for currents in the  $ab$  plane for  $T \lesssim 60$  K, since above  $T_c$  the resistance is considerably larger for currents perpendicular to the  $ab$  plane than in the plane. YBCO conducts principally in the  $ab$  planes. The reason for this unusual behavior is that  $\tau(T) \approx \text{const}$  for temperatures below  $\sim 30$  K for all three axes. One can show that the quasiparticle density at low temperatures is much smaller and increases much slower for the  $c$  axis than for the  $a$  axis or  $b$  axis.

Our model has the following distinct features: (i) the superelectron density  $n_s(T) \propto \lambda(T)^{-2}$  with  $n_s(T) + n_n(T) = \text{const}$ , (ii) the electron scattering rate  $\tau(T)^{-1} \propto \rho_r + T^5 f(T)$  is independent of frequency at microwave frequencies, at least for the temperature interval  $0 < T \lesssim 1.2T_c$ , with the inherent residual resistivity  $\rho_r$  temperature independent, and  $f(T)$  related to the Bloch-Grüneisen  $T$ -dependent resistivity. Since for the present YBCO specimen  $\Theta_D \gg T_c$ , we could have put  $g(t) = 1$  in Eqs. (2), (5), and (6). This simplification affects mainly the minimum in Fig. 2 for both

the  $a$  axis and the  $b$  axis. Since  $r > 1$ , it does not change noticeably the  $c$ -axis results.

We do not draw any conclusions regarding the normal-state resistance above  $\sim 1.2T_c$ . In our model,  $\lambda(T)$  and  $\sigma_{dc}(T_c)$  are experimental (measured) quantities. It does not matter whether the slope of  $\lambda(T)$  is finite or zero at  $T = 0$  K. The value of  $\rho_r$  (or  $r$ ), which is a measure of the inherent residual resistivity at low temperatures, can also be obtained from experiments. The model that we have used adopts an intrinsic electron-scattering rate proportional to  $T^5 f(T)$ , as for scattering by phonons in the Bloch-Grüneisen theory of the normal state, and, as we have seen, it does give rise to a good fit to  $R_s(T)$  in the superconducting state of YBCO. However, the door is wide open on why this fit works as well as it does, since the scattering mechanism in the superconducting state of YBCO is not yet understood. This remains an open question.

The present two-fluid analysis of YBCO is limited to the experiments of Ref. 13 with some numerical information taken from Refs. 12, 14, and 15. It is possible that other cuprates have different temperature dependences of  $\lambda(T)$  than used here. Nevertheless, the present model should be a useful guide for investigations of anisotropy of other cuprates at microwave frequencies. This analysis should also be helpful for future microscopic studies of  $\lambda(T)$ ,  $\tau(T)$ , and the inherent residual resistivity  $\rho_r$  of YBCO and perhaps other cuprates.

- 
- <sup>1</sup>M.R. Trunin, A.A. Zhukov, G.E. Tsydynzhapov, A.T. Sokolov, L.A. Klinkova, and N.V. Barkovskii, *Pis'ma Zh. Eksp. Teor. Fiz.* **64**, 783 (1996) [*JETP Lett.* **64**, 832 (1996)].
- <sup>2</sup>M.R. Trunin, A.A. Zhukov, G.A. Emel'chenko, and I.G. Naumenko, *Pis'ma Zh. Eksp. Teor. Fiz.* **65**, 893 (1997) [*JETP Lett.* **65**, 938 (1997)].
- <sup>3</sup>H.J. Fink, *Phys. Rev. B* **58**, 9415 (1998); **61**, 6346 (2000).
- <sup>4</sup>M.R. Trunin, *J. Supercond.* **11**, 381 (1998); *Usp. Fiz. Nauk* **168**, 931 (1998) [*Phys. Usp.* **41**, 843 (1998)].
- <sup>5</sup>H.J. Fink and M.R. Trunin, *Physica B* **284-288**, 923 (2000).
- <sup>6</sup>M.R. Trunin, Yu.A. Nefyodov, and H.J. Fink, cond-mat/9911211 (unpublished).
- <sup>7</sup>S. Kamal, D.A. Bonn, N. Goldenfeld, P.J. Hirschfeld, R. Liang, and W.N. Hardy, *Phys. Rev. Lett.* **73**, 1845 (1994).
- <sup>8</sup>H. Kitano, T. Shibauchi, K. Uchinokura, A. Maeda, H. Asaoka, and H. Takei, *Phys. Rev. B* **51**, 1401 (1995).
- <sup>9</sup>J. Mao, D.H. Wu, J.L. Peng, R.L. Greene, and S.M. Anlage, *Phys. Rev. B* **51**, 3316 (1995).
- <sup>10</sup>D.A. Bonn, S. Kamal, K. Zhang, R. Liang, and W.N. Hardy, *J. Phys. Chem. Solids* **56**, 1941 (1995).
- <sup>11</sup>H. Srikanth, Z. Zhai, S. Sridhar, and A. Erb, *J. Phys. Chem. Solids* **59**, 2105 (1998).
- <sup>12</sup>S. Kamal, R. Liang, A. Hosseini, D.A. Bonn, and W.N. Hardy, *Phys. Rev. B* **58**, 8933 (1998).
- <sup>13</sup>A. Hosseini, S. Kamal, D.A. Bonn, R. Liang, and W.N. Hardy, *Phys. Rev. Lett.* **81**, 1298 (1998).
- <sup>14</sup>D.N. Basov, R. Liang, D.A. Bonn, W.N. Hardy, B. Dabrowski, M. Quijada, D.B. Tanner, J.P. Rice, D.M. Ginsberg, and T. Timusk, *Phys. Rev. Lett.* **74**, 598 (1995).
- <sup>15</sup>J.L. Tallon, C. Bernhard, U. Binniger, A. Hofer, G.V.M. Williams, E.J. Ansaldo, J.I. Budnick, and Ch. Niedermayer, *Phys. Rev. Lett.* **74**, 1008 (1995).
- <sup>16</sup>P.A. Lee, *Phys. Rev. Lett.* **71**, 1887 (1993).